

CrystEngComm

Accepted Manuscript



This is an *Accepted Manuscript*, which has been through the Royal Society of Chemistry peer review process and has been accepted for publication.

Accepted Manuscripts are published online shortly after acceptance, before technical editing, formatting and proof reading. Using this free service, authors can make their results available to the community, in citable form, before we publish the edited article. We will replace this *Accepted Manuscript* with the edited and formatted *Advance Article* as soon as it is available.

You can find more information about *Accepted Manuscripts* in the [Information for Authors](#).

Please note that technical editing may introduce minor changes to the text and/or graphics, which may alter content. The journal's standard [Terms & Conditions](#) and the [Ethical guidelines](#) still apply. In no event shall the Royal Society of Chemistry be held responsible for any errors or omissions in this *Accepted Manuscript* or any consequences arising from the use of any information it contains.

ARTICLE

Low temperature conversion of titanate nanotubes into nitrogen-doped TiO₂ nanoparticles

Cite this: DOI: 10.1039/x0xx00000x

B. Buchholcz,^a H. Haspel^a, Á. Kukovecz^{a,b,*} and Z. Kónya^{a,c},Received 00th January 2012,
Accepted 00th January 2012

DOI: 10.1039/x0xx00000x

www.rsc.org/

Hydrothermally synthesized protonated titanate nanotubes were doped by nitrogen using ammonia gas as dopant. Thermal decomposition of urea served as ammonia source offering a low-temperature synthesis route for obtaining a potential visible-light photocatalyst. Nitrogen doping could be achieved at as low as 200 °C. The doped samples were calcined at different temperatures and changes in morphology and crystalline phase were studied by transmission and scanning electron microscopy, selected area electron diffraction, energy dispersive X-ray spectroscopy and X-ray diffraction. Nitrogen content and calcination temperature were found to affect the size and shape of the particles as well as their crystalline phase to a great extent. H-form trititanate was showed to transform to rutile TiO₂ through the anatase phase in parallel with the collapse of the nanotube morphology and the production of first rod-like then finally round nitrogen-doped nanoparticles. A phase map was constructed from the data to facilitate the rational design of N-doped trititanate nanotube based nanostructures.

Introduction

In 1998 Kasuga et al.¹ first reported about the preparation of nanotubes from TiO₂ in alkaline media via a hydrothermal process and later Peng et al.² identified the product as a layered trititanate structure (Na_xH_{2-x}Ti₃O₇). In the past decade titanate nanotubes (TiONTs) have attracted considerable attention³ because of their potential use as adsorbents,⁴ ion-exchangers,⁵ lithium-ion batteries,⁶ electrochemical devices,⁷ mesoporous catalyst supports with comparatively large specific surface area and pore volume^{8,9} as well as uses in biomedical applications¹⁰ and photocatalysis.^{11,12}

Both titanate nanotubes and the precursor titanium dioxide are built up of TiO₆ octahedra.¹³ Since TiO₂ has a relatively large indirect band gap energy (3.0 eV in rutile and 3.2 eV in anatase with larger electron mobility¹⁴), its use as photocatalyst is limited to the UV range of the solar light.¹⁵ Large efforts have recently been made to improve the photocatalytic applicability: TiO₂ can be decorated easily with semiconductor nanoparticles, e.g., quantum dots¹⁶ with regulated exciton Bohr radius or can be sensitized with CdS¹⁷ or CdSe¹⁸ nanoparticles, to name a few. Another approach towards photosensibilization is the size¹⁹ and/or shape^{20,21} control. These controlled nanoparticles are of great importance because of their selective catalytic and optical properties.²² Anatase nanoparticles with controlled size and shape were synthesized hydrothermally at 170 °C,²³ and nanobipyramids with the microemulsion method at 250 °C.²⁴

The most common method to prepare TiO₂ with good photocatalytic activity is doping or co-doping it²⁵ with transition metal cations, e.g., Fe³⁺, Mo⁵⁺, Ru³⁺, Os³⁺, Re⁵⁺, V⁴⁺, Rh³⁺,²⁶ and Cr³⁺,²⁷ and/or non-metal elements,²⁸ for instance, B, C, N, S.^{29,30,31,32} Nitrogen-doped (N-doped) titanium-oxides are able to enhance the degradation of organic pollutants in the visible range of solar light.^{33,34} In addition they also have better thermal stability³⁵ than their metal-doped counterparts. However, the lowest temperature synthesis of N-doped titanium oxide nanoparticles with outstanding photocatalytic activity ever reported was 500 °C.³⁶ A real low-temperature route would open up new horizons in the controlled synthesis of such active nanosystems.

TiONTs have even wider band gap energy than the precursor TiO₂. According to Bavykin et al.,³⁷ it equals that of the two-dimensional trititanate sheet (3.87 eV). To increase the photocatalytic activity of TiONTs their structure can be transformed to anatase phase by heat treatment while leaving the tubular morphology intact. When calcined in air, semiconductor nanoparticles have a tendency to be oxidized.³⁸ Thus, heat treatment has to be applied before the material is decorated with photosensibilizer particles. Furthermore, the dopant metal ions influence on the structure and stability of the product nanostructures,³⁹ therefore, the structural and morphological characterization of modified tubular photocatalysts is of vital importance.

There are several ways to obtain N-doped titanate nanotubes (N-TiONTs). Jiang et al.⁴⁰ synthesized N-TiONTs via solvothermal method using NH_4Cl as dopant. Chang et al.⁴¹ exploited the ion-exchange capacity of the titanate nanotubes by changing Na^+ to NH_4^+ with subsequent calcination to TiO_2 . Zhou et al.⁴² prepared first nitrogen-doped TiO_2 and used it as precursor for the Kasuga synthesis,⁴³ Li et al.⁴⁴ reported tubular TiO_2 synthesis via hydrothermal method using ammonium-exchanged potassium hexatitanate nanowires as precursor and Chen et al.²⁹ kept titanate nanobelts in ammonia flow for hours at high temperature.

We developed a method that allows incorporating nitrogen into titanate nanotubes at low temperature (200 °C) in a controlled manner. The nitrogen source is ammonia gas formed *in situ* by the thermal decomposition of urea. In this study we examine the effects of nitrogen doping on the structure and stability of hydrothermally synthesized protonated titanate nanotubes and suggest an approximate phase diagram for nitrogen doped titanate derivatives. To the best of our knowledge, this is the first report on converting titanate nanotubes into nitrogen-doped nanoparticles in a controlled manner at such a low temperature.

Experimental

Synthesis of titanate nanotubes

Titanate nanotubes (TiONTs) were prepared by the combination of the hydrothermal syntheses of Kasuga¹ and Horváth.⁴⁵ In a typical process, 50 g of titanium(IV) oxide powder (99.8% anatase, Sigma-Aldrich) and 1 L 10 M NaOH (99.93%, Molar) were mixed for 1 hour. The obtained white suspension was transferred into a polytetrafluoroethylene (PTFE)-lined stainless steel autoclave (diameter 120 mm, height 250 mm) and kept at 130 °C for 24 hours while rotating the autoclave continuously at 3 rpm around its short axis. The as-prepared white material was washed with 0.01 M HCl (Molar) to neutral pH and finally, the remaining NaCl was washed out with deionized water. The resulting H-form TiONTs were dried in air at 60 °C for 48 hours.

Preparation of nitrogen doped titanate nanotubes

Ammonia gas prepared by the thermal decomposition of urea served as dopant source. 1 g TiONT and 12 g urea (99.46%, Molar) were put into a 400 mL PTFE-lined stainless steel autoclave in the two voids of a hourglass-shaped ceramic sample holder equipped with holes along its perimeter, assembled from laboratory porcelain crucibles (CoorsTek Inc.). The distance between the sample holder and inner surface of the PTFE lining was 1 cm. The whole setup was kept at 200 °C for varied synthesis times of 2, 4, 8, 12 and 24 hours. The estimated pressure of the NH_3 gas in the autoclave was 130 Pa. After doping, the N-doped and the pristine materials underwent a thermal annealing process at elevated temperatures between 400 °C and 900 °C for 1 hour. The product materials were characterized after each annealing step.

Characterization

The structure and morphology of pristine and nitrogen-doped samples was characterized by transmission electron microscopy (TEM) and selected area electron diffraction (SAED) using a FEI Tecnai G² 20 X-Twin instrument (200 kV accelerating voltage). The samples were drop-casted from ethanol suspension onto copper mounted holey carbon grids. Scanning electron microscopy (SEM) observations and energy dispersive X-ray spectroscopy (EDS) measurements were carried out on a HITACHI S-4700 Type II instrument (30 kV accelerating voltage) equipped with a Röntec QX2 energy dispersive X-ray spectrometer. The crystal structure was examined by a Rigaku Miniflex II powder X-ray diffractometer using $\text{Cu K}\alpha$ radiation source ($\lambda = 0.15418$ nm) operating at 30 kV and 15 mA at room temperature. A scanning rate of 4 degrees/min in the 5–60° 2 θ range was used.

Results and discussion

Particle size and morphology

Figures 1a–f illustrate the morphological transition of TiONTs during nitrogen doping before any heat treatment. Inset graphs depict SAED patterns. The hydrothermally synthesized titanate nanotubes are open-ended tubular objects with a length of 110–120 nm having 6–7 nm inner and 14–15 nm outer diameters as shown in Figure 1a. The effect of increasing the doping time is depicted in Figures 1b–f. Nitrogen doping for 2 and 4 h left the tubular morphology intact (Figures 1b–c). After doping for 8 h approximately 25 nm long crystals and tube fragments were obtained besides the remaining nanotubes in Figure 1d, and after 12 h the nanotubes collapsed as depicted in Figures 1e–f. Increasing the synthesis time above 12 h converted the tubular morphology into cubes and octahedrons of 20–30 nm edge length. According to the SAED analysis, after N-doping for 2 and 4 h the samples exhibited the same diffractions as pristine TiONTs. Diffractions characteristic of the anatase phase TiO_2 appeared in the diffraction pattern after 8 h doping and became dominant when the ammonia treatment was longer than 12 h as shown in Figures 1e–f. No rutile phase could be detected under the applied synthesis conditions,³ i.e. without any subsequent high-temperature calcination.

The nitrogen content of the doped TiONT samples was determined by EDS elemental analysis and found to be 0.11, 0.13, 0.7, 6.3 and 6.6 atom% in the 2, 4, 8, 12 and 24 h doped samples, respectively. These values correlate well with recent X-ray photoelectron spectroscopic studies^{43,46,47} that reported 0.5–2.5 atomic percent nitrogen in various doped titanium-oxide nanostructures. Two different sites were suggested to be available for nitrogen incorporation in the titania structure. According to Bertóti et al., oxygen can be substituted by nitrogen up to a metal to nitrogen ratio of as high as 0.6.⁴⁸ Alternatively, nitrogen can be present at Ti-O-N sites^{43,46,47} as well. The ammonia gas molecules used as dopant source in the present study may reside in the interlayer space of the nanotube walls, be adsorbed on the tube surface or initiate the

transformation into ammonium-titanate.⁴¹⁻⁴³ The phase transformation in the cases of the 12 and 24 h doped samples can also be effected by the pressure of the ammonia gas between the tube layers or by a similar transformation as reported by Li et al.⁴⁴

Heat treatment affects the crystal structure of titanate nanotubes^{49,50} transforming them into rutile TiO₂ through the anatase phase^{51,52} at high temperatures. In order to link the structural changes (discussed in the next section below) with morphological transformations we studied the effect of doping duration on the TEM-derived average particle length in both as-synthesized samples and in TiONTs calcined at 400, 600 and 900 °C for 1 hour. Figure 1g summarizes the results of this analysis (original TEM images are not shown). Lines in the figure are guides for the eye.

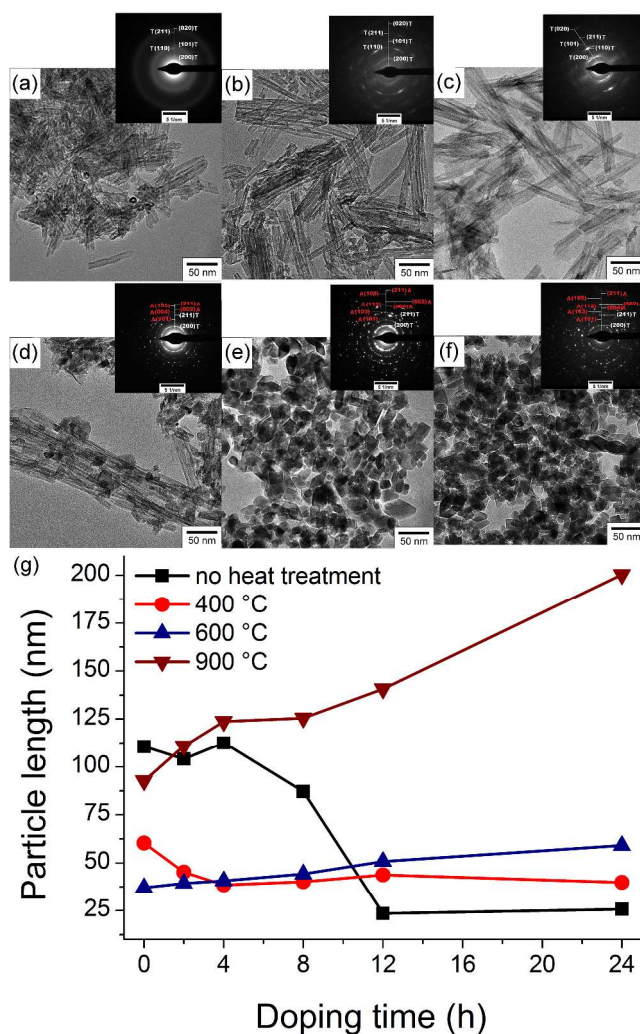


Figure 1. TEM images and SAED patterns of pristine (a) and nitrogen-doped samples after 2 h (b), 4 h (c), 8 h (d), 12 h (e) and 24 h (f) doping. "T" and "A" denote diffractions assigned to the trititanate and the anatase phase, respectively. Part (g) depicts the variation of the average particle length with nitrogen doping time in TiONTs samples calcined at temperatures indicated in the legend for 1 hour. Lines in panel g) are only guides for the eye.

The average particle length of the untreated sample decreased from the starting value of ~110 nm to 85 nm after 8 h of

nitrogen doping. At this particular synthesis time both tubular and isomorphic particles were observable in the TEM images of Figure 1d. After 12 h doping the average particle size dropped to 25 nm and remained constant with further increase in doping time. The disappearance of the original tubular structure was visible in Figures 1e-f. Samples calcined at 400 and 600 °C behaved similarly during the heat treatment insofar as the particle size was reduced but the nitrogen doping had little additional effect. The initial rod-like morphology gradually transformed to isomorphic particles after 2 h doping at 400 °C and without any nitrogen content at 600 °C and above. The particle size in the samples calcined at 900 °C increases monotonously from the initial value of 95 nm to about 200 nm with increasing nitrogen doping time.

The effects of nitrogen doping and subsequent calcination steps on the shape of the TiONT-derived nanostructures were assessed by quantitative particle roundness analysis of SEM images. Typical SEM images are shown in Figure 2a for pristine nanotubes and in Figure 2b-d for samples calcined at 400 °C, 600 °C and 900 °C, respectively.

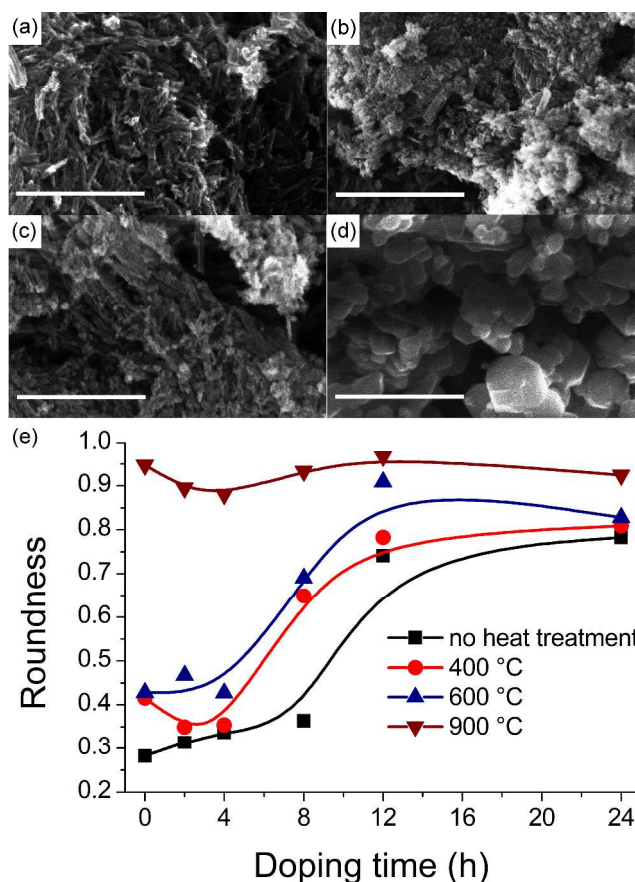


Figure 2. Typical SEM images of pristine (a) and calcined TiONTs heat treated at 400 °C (b), 600 °C (c) and 900 °C (d). The scale bar is 500 nm in all figures. Part (e) depicts the variation of roundness as a function of nitrogen doping at different calcination temperatures. Lines in panel e) are guides for the eye.

Roundness C as defined in eq 1 is a shape descriptor parameter.^{53,54}

$$C = \frac{4 \cdot \pi \cdot A}{P^2} \quad (1)$$

Here A is the projected area of a particle and P is the perimeter of this area. The roundness of a perfect circle is 1. The smaller the roundness value, the larger is the difference between the perfect circle shape and the projected shape of the actual nanoobject. Figure 2e summarizes the effects of nitrogen doping and calcination temperature on TiONT roundness.

It can be seen that both nitrogen doping and heat treatment affect the shape of the particles. As-synthesized TiONTs are one-dimensional nanostructures; therefore, their initial roundness is low (0.28) and increases gradually to 0.35 in the first 8 hours as nitrogen doping transforms the structure. After 8 hours a steep rise occurs and roundness stabilizes at ~ 0.75 for long doping times. The general roundness character of TiONTs calcined at 400 °C and 600 °C is similar, however, the steep roundness increase is shifted towards lower doping times with higher calcination temperature. The projected shape of samples calcined at 900 °C is almost perfectly circular (~ 0.95) and is largely unaffected by doping time.

Summarizing, longer ammonia treatment and higher calcination temperature promote the shape-shifting of tubular trititanates into isotropic nanoparticles. The reason for this phenomenon is that both N-doping and elevated temperature interact directly with the lamellar trititanate structure and facilitate the destruction of trititanate nanotubes. These two effects can partially compensate each other and this is the reason for the shifting of the roundness curve towards lower doping times with higher temperature. When calcined at 900 °C, the material recrystallizes completely due to temperature effects alone, therefore, nitrogen doping duration has no additional effect on the roundness value.

The exact mechanism of nitrogen-induced trititanate destruction has not been elucidated yet. Chang et al. have identified⁴¹ several ways for NH_3 to interact with the wall structure in ammonium-trititanate nanotubes including low temperature (300 °C) pressure related tube fracture and the formation of interstitial NH_2 species on the nanotube wall at 400 °C. In our case the temperature is lower (200 °C) during the doping, but the heat treatment is typically longer (2-12 h in this work vs. 3 h in Ref. 41). Therefore, it is possible that the same breakdown mechanisms also work here. Moreover, since ammonia in our system is formed by the thermal decomposition of urea, it is also possible that some other volatile decomposition products (either isocyanic acid which is a primary decomposition product, or CO_2 which is produced when isocyanic acid reacts with the water content of the nanotubes) also play a role in trititanate destruction.

Characterization of the phase transformation

The transformation from trititanate to anatase/rutile phase was investigated by XRD measurements. Figure 3 shows the effect of nitrogen doping on the crystalline structure of untreated TiONTs samples (Figure 3a) and on those calcined at 400 °C, 600 °C and 900 °C (Figures 3b-d), respectively. In Figure 3a the diffraction pattern of the undoped TiONTs agrees well with previous literature results,^{11,12,45} After 8 h nitrogen doping anatase reflections (JCPDS card No. 21-1272) appear besides the remaining trititanate reflections that diminish with increasing synthesis time. Samples calcined at 400 °C and 600 °C (Figures 3b-c) exhibit only reflections characteristic to anatase even without any nitrogen doping. The narrowing of the (101) anatase reflection ($2\theta = 25.7^\circ$) in Figures 3b-c implies a higher crystallization degree at elevated heat treatment temperatures. At the calcination temperature of 900 °C (Figure 3d) rutile reflections (JCPDS card No. 21-1276) show up besides those assigned to the anatase phase. The increase in the intensity of the (110) rutile reflection ($2\theta = 27.8^\circ$) with ongoing nitrogen doping indicates a phase transition induced by the insertion of nitrogen into the structure.

In order to quantitatively characterize the variation of the crystallization degree as a function of nitrogen doping, anatase crystallite size was calculated by the Scherrer-equation⁵⁵ from the (101) reflection of the anatase phase:

$$L = \frac{K \cdot \lambda}{\beta \cdot \cos \Theta} \quad (2)$$

where K is a numerical constant taken as 0.9, λ is the X-ray wavelength, β is the full width at half-maximum (FWHM) of the investigated reflection and θ is the diffraction angle. Results, i.e., the variation of anatase crystallite size with nitrogen doping time are depicted in Figure 4.

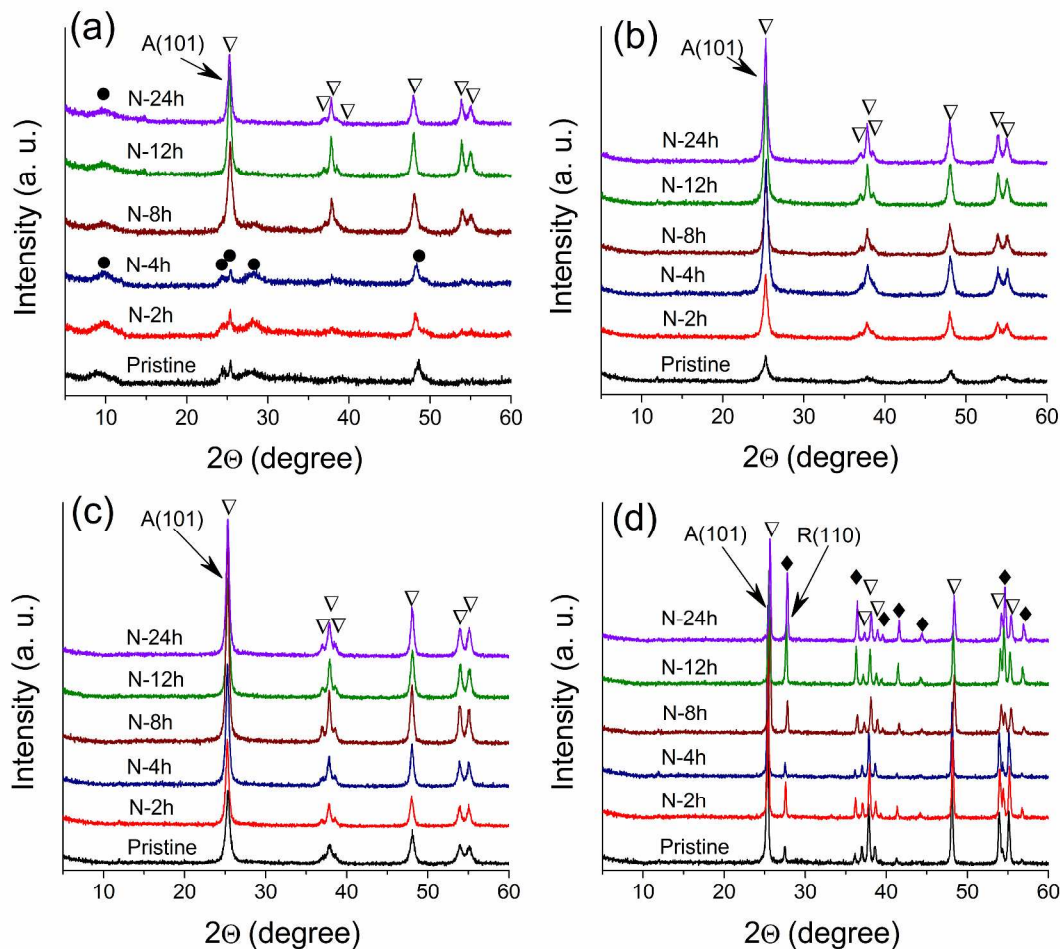
It is clearly seen that anatase crystallite size increases monotonously with the heat treatment temperature in the undoped samples from 10 nm to about 40 nm. Below the calcination temperature of 800 °C two hours of nitrogen doping is sufficient to obtain the final crystallite sizes 15-25 nm. At 800 °C the crystallite size starts to decrease after an initial rise of 4 h synthesis time, and reaches its final size of ~ 27 nm at 12 h. At 900 °C, crystallite size between 38 and 48 nm increases gradually also reaches its final size already at 12 h. To get further quantitative information about the phase transformation from anatase to rutile, the rutile weight fraction was calculated for the nitrogen-doped samples calcined at 900 °C from the integrated peak areas of the rutile (110) reflection:⁵⁶

$$W_R = \frac{A_R}{0.884 \cdot A_A + A_R} \quad (3)$$

where A_R is the integrated intensity of the rutile (110) reflection, A_A is the integrated intensity of the anatase (101) and 0.884 is a previously suggested value of a coefficient.⁵⁷ The dashed line in Figure 4 shows the rutile weight fraction in percentage.

The rutile content of the sample calcined at 900 °C increases monotonously with ongoing nitrogen doping from ~7% to 40%.

These results imply that higher nitrogen content largely facilitates the phase transition from trititanate to anatase as it is seen in Figure 3a, and further from anatase to rutile at elevated temperatures as evidenced in Figures 3b–d and Figure 4.



F

Figure 3. Variation of the XRD pattern of TiONTs before heat treatment (a) and calcined at 400 °C (b), 600 °C (c) and 900 °C (d). Reflections assigned to trititanate nanotubes “●”, anatase “▽” and rutile “◆” are indicated in each panel.

ARTICLE

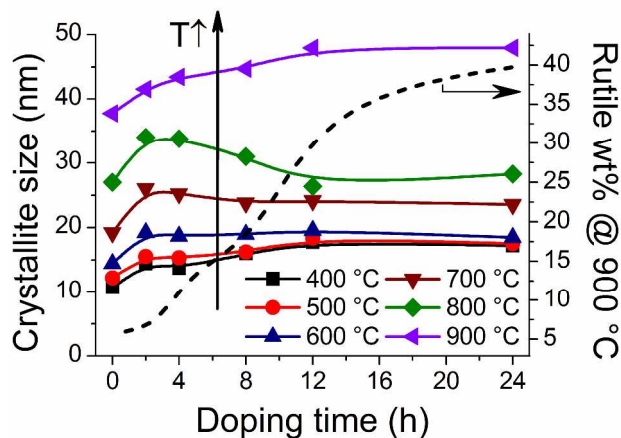


Figure 4. Variation of the anatase crystallite size with nitrogen doping under different calcination conditions (left axis), and the rutile weight fraction in the sample calcined at 900 °C (right axis). Lines are guides for the eye.

All these results can be summarized in the diagram shown in Figure 5 where the morphological and phase transitions of trititanate nanotubes are presented as functions of nitrogen doping duration and calcination temperature. This phase map allows the rational planning of experiments that yield a particular crystalline phase and morphology of product titanium-oxide material.

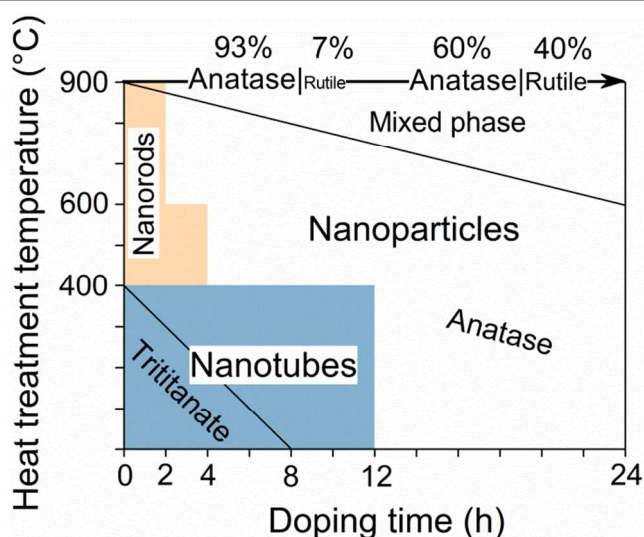


Figure 5. Variation of the morphology and crystalline phase of the nitrogen-doped titanium-oxide nanostructures with nitrogen-dotation and calcination temperature.

Figure 5 confirms that N-doped trititanate nanotubes are only stable at relatively low nitrogen content and temperature. The incorporation of nitrogen into the structure and the application of a high-temperature calcination step both facilitate the transformation of the trititanate phase to anatase and forth to rutile. Nanotubes are converted first into rod-like and then to isotropic nanoparticles during the process.

Conclusions

H-form titanate nanotubes were prepared by the alkaline hydrothermal method and subsequently doped by nitrogen obtained from the thermal decomposition of urea. The developed method offers the lowest temperature route to N-doped trititanate-derived nanostructures reported until now. The amount of incorporated nitrogen could be controlled by the duration of the reaction. Nitrogen in high concentration induced both structural and morphological changes even without any additional heat treatment. However, by calcining the doped samples it was possible to facilitate nitrogen-related transitions in the oxide morphology and crystalline phase, resulting in materials with higher crystallinity and more regular shape. A visual phase map was constructed to rationalize the synthesis of nitrogen doped titanium oxide nanostructures with desired shape and crystalline structure using tubular trititanate precursors.

Acknowledgements

The financial support of the TÁMOP-4.2.2.A-11/1/KONV-2012-0047, TÁMOP-4.2.2.A-11/1/KONV-2012-0060 and OTKA NN 110676 projects is acknowledged.

Notes and references

^a Department of Applied and Environmental Chemistry, University of Szeged, H-6720 Szeged, Rerrich Béla tér 1, Hungary.

^b MTA-SZTE "Lendület" Porous Nanocomposites Research Group, H-6720 Szeged, Rerrich Béla tér 1, Hungary.

^c MTA-SZTE Reaction Kinetics and Surface Chemistry Research Group, H-6720 Szeged, Rerrich Béla tér 1, Hungary.

* Corresponding author email: kakos@chem-szeged.hu (Á. Kukovecz)

- 1 T. Kasuga, M. Hiramatsu, A. Hoson, T. Sekino and K. Niihara, *Langmuir* 1998, **4**, 3160.
- 2 Q. Chen, G.H. Du, S. Zhang and L.M. Peng, *Acta. Cryst. Sect. B* 2002, **58**, 587.
- 3 D.V. Bavykin and F.C. Walsh, *Titanate and titania nanotubes: synthesis, properties and applications*, RSC: Cambridge, 2010.
- 4 D.V. Bavykin, A.A. Lapkin, P.K. Plucinski, J.M. Friedrich and F.C. Walsh, *J. Phys. Chem. B* 2005, **109**, 19422.
- 5 D.V. Bavykin and F.C. Walsh, *J. Phys. Chem. B* 2007, **111**, 14644.
- 6 L. Kavan, M. Kalbac, M. Zukulová, I. Exnar, V. Lorenzen, R. Nesper and M. Graetzel, *Mater. Chem. Mater.* 2004, **16**, 477.
- 7 G. Jian, Q. Hu, S. Lu, D. Zhou and Q. Fu, *Processing and Application of Ceramics* 2012, **6**, 215.
- 8 D.V. Bavykin, V.N. Parmon, A.A. Lapkin and F.C. Walsh, *J. Mater. Chem.* 2004, **14**, 3370.
- 9 E.E. Kiss and G.C. Boskovic, *Processing and Application of Ceramics* 2012, **6**, 173.
- 10 A. Liu, M. Wei, I. Honma and H. Zhou, *Anal. Chem.* 2005, **77**, 8068.
- 11 M. Hodos, E. Horváth, H. Haspel, Á. Kukovecz, Z. Kónya and I. Kiricsi, *Chem. Phys. Lett.* 2004, **399**, 512.
- 12 Á. Kukovecz, M. Hodos, Z. Kónya and I. Kiricsi, *Chem. Phys. Lett.* 2005, **411**, 445.
- 13 Á. Kukovecz, M. Hodos, E. Horváth, G. Radnóczy, Z. Kónya and I. Kiricsi, *J. Phys. Chem. B* 2005, **109**, 17781.
- 14 H. Tang, K. Prasad, R. Sanjines, P.E. Schmid, and F. Levy, *J. Appl. Phys.* 1994, **75**, 2042.
- 15 A.L. Linsebigler, G. Lu and J. Jr. Yates, *Chem. Rev.* 1995, **95**, 735.
- 16 A. Kongkanand, K. Tvrđy, K. Takechi, M. Kuno and P.V. Kamat, *J. Am. Chem. Soc.* 2008, **130**, 4007.
- 17 Y. Tachibana, K. Umekita, Y. Otsuka and S. Kuwabata, *J. Phys. Chem. C* 2009, **113**, 6852.
- 18 J. Kim, S. Choi, J. Noh, S. Yoon, S. Lee, T. Noh and K. Hong, *Langmuir* 2009, **25**, 5348.
- 19 C. Aprile, A. Corma and H. Garcia, *Phys. Chem. Chem. Phys.* 2008, **10**, 769.
- 20 Y.W. Jun, M.F. Casula, J.H. Sim, S.Y. Kim, J. Cheon and A.P. Alivisatos, *J. Am. Chem. Soc.* 2003, **125**, 15981.
- 21 Z. Bian, T. Tachikawa and T. Majima, *J. Phys. Chem. Lett.* 2012, **3**, 1422.
- 22 B. Shao, Q. Zhao, N. Guo, Y. Jia, W. Iv, M. Jiao, W. Lü and H. You, *Cryst. Growth Des.* 2013, **13**, 3582.
- 23 Y. Mao and S.S. Wong, *J. Am. Chem. Soc.* 2006, **128**, 8217.
- 24 C. Chen, R. Hu, K. Mai, Z. Ren, H. Wang, G. Qian and Z. Wang, *Cryst. Growth Des.* 2011, **11**, 5221.
- 25 E.W. McFarland and H. Metiu, *Chem. Rev.* 2013, **113**, 4391.
- 26 W. Choi, A. Termin and M.R. Hoffmann, *J. Phys. Chem.* 1994, **98**, 13669.
- 27 E. Borgarell, J. Kiwi, M. Graetzel, E. Pelizzetti and M. Visca, *J. Am. Chem. Soc.* 1982, **104**, 2996.
- 28 J. Zhang, Y. Wu, M. Xing, S.A.K. Leghari and S. Sajjad, *Env. Eng. Sci.* 2010, **3**, 715.
- 29 X. Chen and C. Burda, *J. Am. Chem. Soc.* 2008, **130**, 5018.
- 30 V. Likodimos, C. Han, M. Pelaez, A.G. Kontos, G. Liu, D. Zhu and P. Falaras, *Ind. Eng. Chem. Res.* 2013, **52**, 13957.
- 31 D. Chen, Z. Jiang, J. Geng, Q. Wang and D. Yang, *Ind. Eng. Chem. Res.* 2007, **46**, 2741.
- 32 K. Yang, Y. Dai and B. Huang, *J. Phys. Chem. C* 2007, **111**, 18985.
- 33 Y. Wang, C. Feng, M. Zhang, J. Yang and Z. Zhang, *Appl. Catal. B* 2010, **100**, 84.
- 34 Y. Wang, C. Feng, M. Zhang, J. Yang and Z. Zhang, *Appl. Catal. B* 2011, **104**, 268.
- 35 Y. Cong, J. Zhang, F. Chen and M. Anpo, *J. Phys. Chem. C* 2007, **111**, 6976.
- 36 H. Ou, S. Lo and C. Liao, *J. Phys. Chem. C* 2011, **115**, 4000.
- 37 D.V. Bavykin, S.N. Gordeev, A.V. Moskalenko, A.A. Lapkin and F.C. Walsh, *J. Phys. Chem. B* 2005, **109**, 8565.
- 38 L. Qi, H. Cölfen and M. Antonietti, *Nano Letters* 2001, **1**, 61.
- 39 A. Rónavári, B. Buchholz, Á. Kukovecz and Z. Kónya, *J. Mol. Struct.* 2013, **1044**, 104.
- 40 Z. Jiang, F. Yang, N. Luo, B.T. Chu, D. Sun, H. Shi and P.P. Edwards, *Chem. Comm.* 2008, **47**, 6372.
- 41 J.C. Chang, W.J. Tsai, T.C. Chiu, C.W. Liu, J.H. Chao and C.H. Lin, *J. Mater. Chem.* 2011, **21**, 4605.
- 42 Q. Zhou, J. Mao, J. Xiao and G. Xie, *Anal. Methods* 2010, **2**, 1063.
- 43 J. Wang, D.N. Tafen, J.P. Lewis, Z. Hong, A. Manivannan, M. Zhi and N. Wu, *J. Am. Chem. Soc.* 2009, **131**, 12290.
- 44 J. Li, Y. Yu, Q. Chen, J. Li and D. Xu, *Cryst. Growth. Des.* 2010, **10**, 2111.
- 45 E. Horváth, Á. Kukovecz, Z. Kónya and I. Kiricsi, *Chem. Mater.* 2007, **19**, 927.
- 46 L. Gai, X. Duan, H. Jiang, Q. Mei, G. Zhou, Y. Tian and H. Liu, *CrystEngComm* 2012, **14**, 7662.
- 47 P. Dong, Y. Wang, B. Liu, L. Guo, Y. Huang and S. Yin, *S. J. Am. Ceram. Soc.* 2012, **95**, 82.
- 48 I. Bertóti, *Catal. Today* 2012, **181**, 95.
- 49 G. Pótári, D. Madarász, L. Nagy, B. László, A. Sági, A. Oszkó and J. Kiss, *Langmuir* 2013, **29**, 3061.

-
- 50 P. Szirmai, E. Horváth, B. Náfrádi, Z. Micković, R. Smajda, D.M. Djokić, K. Schenk, L. Forró and A. Magrez, *J. Phys. Chem. C* 2013, **117**, 697.
- 51 D.V. Bavykin, J.M. Friedrich and F.C. Walsh, *Adv. Mater.* 2006, **18**, 2807.
- 52 J. Li, Z. Tang and Z. Zhang, *Chem. Mater.* 2005, **17**, 5848.
- 53 E.P. Cox, *J. Paleontol.* 1927, **1**, 179.
- 54 K.A. Alshibli and M.I. Alsaleh, *J. Comp. In. Civ. Engrg.* 2003, **18**, 36.
- 55 A.L. Patterson, *Phys. Rev.* 1939, **56**, 978.
- 56 H. Zhang and J.F. Banfield, *J. Phys. Chem. C* 2000, **104**, 3481.
- 57 A.A. Gribb and J.F. Banfield, *Am. mineral.* 1997, **82**, 717.

Table of contents entry for manuscript CE-ART-04-2014-000801 “Low temperature conversion of titanate nanotubes into nitrogen-doped TiO₂ nanoparticles”

Text:

We report on the record lowest synthesis temperature for nitrogen doped titanate nanostructures and their subsequent conversion into N-doped TiO₂.

Graphic:

